Interlevel nonradiative transitions of impurities in solids

O. Pilla, M. Montagna, and G. Viliani
Dipartimento di Fisica, Universita di Trento, 38050 Povo, Trento, Italy
and Gruppo Nazionale di Struttura della Materia, Trento, Italy
(Received 18 February 1981)

The spin-orbit interaction in transition-metal ions induces fast nonradiative transitions among states of different spin; the transition rates can be directly measured by the homogeneous broadening of zero-phonon optical lines. The configuration-interaction formalism developed by Fano is well suited for the evaluation of the widths and shifts caused by these nonradiative processes. By taking the Jahn-Teller effect into account, we have shown that within the framework of Fano's formalism it is possible to reproduce the shape of the zero-phonon line of $MgO:V^{2+}$ as regards both widths and splittings without making use of any fitting parameter. The model has also been applied to $Al_2O_3:Cr^{3+}$, $Cs_2SiF_6:Mn^{4+}$, and $MgO:Cr^{3+}$; its limits of validity have been discussed.

I. INTRODUCTION

Nonradiative transitions (NRT) in molecules and impurity centers in crystals have recently been the object of increasing interest, both from the theoretical and experimental standpoints.[1-4] Such processes are in general rather difficult to study, especially in solids where transition rates as high as 10^{13} sec^{-1} or more can be reached. In these cases clearly, one is forced to get information about transition rates from indirect measurements such as quantum yields, homogeneous broadening of lines, and so on.

Theoretical difficulties are also rather strong. First of all, in solids, the impurity center in general interacts with many vibrational degrees of freedom of the host crystal, whose frequency is not well defined but rather varies continuously over the range of allowed phonon frequencies. This implies that in most cases the simple cluster model cannot be used even as a first approximation. We shall see in the following sections that this interaction between the electronic states of the impurity and the continuum of vibrational states of the crystal is the key mechanism for nonradiative transitions among different electronic states of the impurity. Another source of trouble is that in most cases, the operators which cause nonradiative transitions, i.e., the nonadiabatic and anharmonic operators, have a fairly complicated form. Last but not least, the excited electronic states of impurities are very often orbitally degenerate; this implies that the Jahn-Teller effect must be taken into account. In this regard, it may be anticipated that one of the interesting results of the present work is showing that, in the cases where NRT have appreciable strength, the well-established theory of Ham's quenching of spin-orbit interaction must be applied with some caution in order to reproduce the experimental results.

Of the above-mentioned theoretical difficulties, however, only the one connected with the poor knowledge of the promoting operators is really basic because one can manage to treat the electron-continuum interaction, even in the presence of Jahn-Teller effect, at least approximately. In this regard, it is very interesting to consider transition-metal ions with the d^3 electronic configuration and their interlevel quadruplet-doublet nonradiative transitions. Actually, for these transitions the nonadiabatic operator alone is ineffective because of the spin change, and the direct spin-orbit-induced NRT is expected to be the most important process. This is a very important point because the matrix elements of the spin-orbit interaction are well known, and it is possible to set up a nonphenomenological theory, as shown briefly in Ref. 5.

By assuming the adiabatic approximation as a starting point, the relaxation process that follows optical excitation of the center, which is vibronically coupled to the host lattice, can be schematized by several successive steps (Fig. 1): In the first step the system thermalizes within the same electronic state releasing the excess energy to the phonon bath of the crystal; in the second the nonradiative transition to the continuum of vibronic states relative to a different electronic state takes place, after which (third

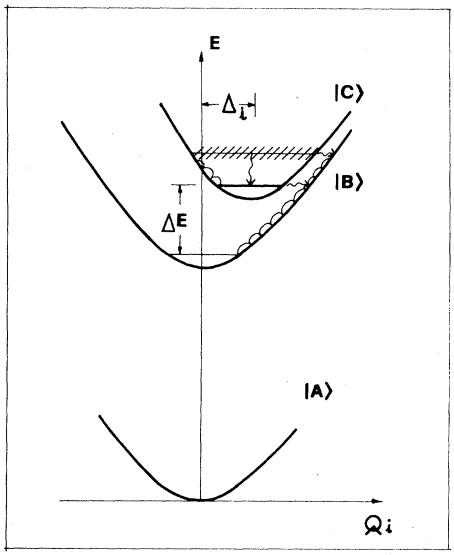

FIG. 1. Schematic energy-level diagram for a three-level system. Wavy arrows indicate interlevel nonradiative transitions; internal relaxation in the excited states is also indicated on the parabolas. The quantities Δ_i and ΔE are defined in the text.

step) thermalization within the second state is accomplished. The transition rates relative to the first two steps may be of the same order of magnitude, so that nonradiative transfer from vibrationally excited states of $|C\rangle$ to $|B\rangle$ may be appreciable. After all this, a photon is emitted and the system goes back to the ground electronic state, where a further vibrational relaxation can possibly take place. This picture is meaningful if competitive processes (such as radiative $|C\rangle \rightarrow |A\rangle$ emission, nonradiative $|B\rangle \rightarrow |A\rangle$ decay, energy transfer to other centers, etc.) are not very important. Moreover, the necessity of introducing such a picture stems from the practical impossibility of solving the Schrödinger equation for the whole (ion + lattice) system; actually, if this could be done there would be no need at all for introducing nonradiative transitions.

As said, typical systems where NRT are important and which can be schematized by the level sequence of Fig. 1 are the 3 d^3 ions, such as V^{2+}, Cr^{3+}, and Mn^{4+} in ionic lattices, where the state $|A\rangle$ corresponds to the $^4A_2$ ground state, $|B\rangle$ represents the $^2T_1$ and ^2E levels, and $|C\rangle$ corresponds to $^4T_2$. The spin-orbit coupling between different states acts as a strong mixing operator inducing NRT among the above-mentioned states. In particular, we will be interested in NRT between the $^4T_2$ and ^2E, $^2T_1$ levels, which are fast enough to give appreciable homogeneous broadening of the $^4T_2$ zero-phonon line ($\sim 10-50$ cm^{-1}).

Actually, an alternative source of (inhomogeneous) broadening of the lines is random strain at the impurity sites; this is the mechanism which broadens at low temperature the $^2E \rightarrow {}^4A_2$ zero-phonon transition, which has a very long lifetime ($\sim$ 10 msec) and a nearly Gaussian shape whose width is $\sim 0.1-0.3$ cm^{-1} in good-quality crystals. In contrast, in MgO:V^{2+} the shape of the $^4A_2 \rightarrow {}^4T_2$ spin-orbit components is Lorentzian and, in the case of ruby, line narrowing is not observed in emission by laser excitation.[6]

The most complete calculation so far performed on Cr^{3+}-like systems is due to Englman and Barnett[7,8] who studied radiative and nonradiative transitions as a function of temperature and of the electron-phonon coupling parameters for a system like the one schematized in Fig. 1. In the framework of the same model, employing a single vibrational mode, Fonger and Struck[9] computed the nonradiative transition rates among the states of Cr^{3+} in ruby and emerald.

The models of Refs. 7–9 are suitable for computing the temperature dependence of the nonradiative transition rates, but cannot give the absolute value of such rates because they involve a phenomenological electronic factor which is used as a fitting parameter. Moreover, such a factor is taken to be the same for all electronic states. Also, the use of a single frequency makes the results of Refs. 7 and 8 strongly dependent on the vibrational energy, giving rise to resonance effects when $E_C(\min) - E_B(\min)$ is a multiple of $\hbar\omega$. A more realistic model has been employed by Sturge[10] in the study of NRT in the two-level system $KMgF_3$:Co^{2+}, by taking into account phonon dispersion.

In the present paper we will take a different approach with respect to Sturge's; in fact, since we are interested in the low-temperature shape of the $^4A_2 \rightarrow {}^4T_2$ zero-phonon line (ZPL), it is more natural to adopt the configuration-interaction approach[11,12] dealing with stationary states which are a mixing of discrete and continuum configurations, and giving further information such as the Lamb-like shift of the discrete levels. We will also introduce the Jahn-Teller effect on the upper level, which will turn out to be essential to account for experimental line shapes.

The results we obtain compare very well with the experimental data of MgO:V^{2+}, whose $^4A_2 \rightarrow {}^4T_2$

zero-phonon line is reasonably well resolved, and of $Al_2O_3:Cr^{3+}$. Comparison with other systems ($MgO:Cr^{3+}$, $Cs_2SiF_6:Mn^{4+}$) is also established and, besides being in reasonable agreement with experiment, it helps to determine the limits of validity of the model and assumptions employed, which will be described in the following sections.

In Sec. II a simplified model for a three-level system, not including the Jahn-Teller effect (JTE), is introduced; the model is checked on $MgO:V^{2+}$ in Sec. III. Section IV is devoted to presenting the theory with JTE and to applying it to the above-mentioned impurity systems.

II. A SIMPLIFIED MODEL FOR NONRADIATIVE TRANSITIONS

In order to focus on the physical origin of the processes which determine the zero-phonon line shape, we shall introduce a simplified model with three electronic levels, whose extension to a more realistic picture will be carried out in the following sections. We shall consider the Fano-type configuration interaction between the zero-phonon state relative to $|C\rangle$ and the continuum of vibronic states relative to the electronic state $|B\rangle$. The assumptions we make are the following:

(1) The three levels A, B, and C of Fig. 1 are not degenerate.

(2) The total Hamiltonian of the system is divided into two parts, $H = H_0 + H'$. The zero-order wave functions are adiabatic products, and H' is a purely electronic operator which couples such wave functions. The electronic wave function $\phi(r)$ does not depend on nuclear coordinates (crude adiabatic approximation).

(3) Only totally symmetrical Γ_1^+ vibrations are considered in linear coupling (i.e., if there were only one vibrational mode as in Fig. 1, the parabolas would all have the same curvature).

(4) The nuclear equilibrium configurations of states $|A\rangle$ and $|B\rangle$ are the same, whereas the one relative to $|C\rangle$ is determined by the displacements Δ_i in the subspaces of the coordinates q_i ($\Delta_i^{AB} = 0$, $\Delta_i^{BC} = \Delta_i^{AC} \neq 0$).

(5) At zero order, radiative transitions are allowed only between states $|A\rangle$ and $|C\rangle$.

For application to Cr^{3+}-like systems, only hypothesis (3) is really limiting and will be partially relaxed in the following sections.

We shall consider the Fano-type configuration interaction between the zero-phonon state relative to $|C\rangle$ and the continuum of vibronic states relative to the electronic state $|B\rangle$. The vibrational states of the continuum will be indicated as

$$|0\rangle = \Pi_i |0_i(Q_i)\rangle \tag{1}$$

for the ground ($n_i = 0$) vibrational states, and

$$|n(\Omega)\rangle = \Pi_i |n_i(Q_i)\rangle \tag{2}$$

for the excited states, where $n = \sum n_i$ is the total number of vibrations present in the state, whose total energy is

$$\hbar\Omega = \hbar \sum_i n_i \omega_i \tag{3}$$

and Q_i is the ith normal coordinate. Since the ω_i's belong to a discrete set of frequencies, it can be assumed that n and Ω determine uniquely the vibrational state; on the other hand, the density of states is so high that the vibrational wave functions obey the continuum orthogonality relation

$$\langle n(\Omega_1) | m(\Omega_2)\rangle = \delta_{nm}\delta(\Omega_1 - \Omega_2) \ .$$

The functions $|n_i(Q_i)\rangle$ are harmonic oscillator wave functions centered on the origin ($Q_i = 0$); the vibronic wave functions and eigenvalues are

$$\begin{aligned} |\psi_A^n(E)\rangle &= |\phi_A\rangle |n(\Omega)\rangle, \quad E = E_A^0 + \hbar\Omega \\ |\psi_A^n(E)\rangle &= |\phi_A\rangle |n(\Omega)\rangle, \quad E = E_A^0 + \hbar\Omega \\ |\psi_B^n(E)\rangle &= |\phi_B\rangle |n(\Omega)\rangle, \quad E = E_B^0 + \hbar\Omega \end{aligned} \tag{4}$$

where the E^0's are the energies of the vibronic states and $|n'\rangle$ is the harmonic oscillator wave function centered on the minimum of level $|C\rangle$ and is related to $|n\rangle$ by

$$|n'(Q_i - \Delta_i)\rangle = |n(Q_i)\rangle \ , \tag{5}$$

where Δ_i is the displacement of the minimum.

The strength of the electron-phonon coupling is given by the Huang-Rhys factor S_0:

$$S_0 = \tfrac{1}{2} \sum_i \Delta_i^2 \ .$$

In order to compute the nonradiative transition rates, we will need the overlap integrals $\langle n | n'\rangle = a_{nn'}$ which also determine the shape of the normalized absorption band $G(\Omega)$. At low temperatures we have

$$G(\Omega) = |a_{00'}|^2 \delta(\Omega) + \sum_{n'=1}^{\infty} |a_{0n'}(\Omega)|^2 \ , \tag{6}$$

where

$$a_{00'} = \langle 0 \mid 0' \rangle, \quad a_{0n'}(\Omega) = \langle 0 \mid n'(\Omega) \rangle \ . \tag{7}$$

The square of the generic matrix element $a_{0n'}(\Omega)$ may be obtained by convoluting $|a_{01'}(\Omega)|^2$, $n-1$ times with itself, which is proportional to the effective phonon spectrum.

We now have to diagonalize the total Hamiltonian $H = H^0 + H'$ between the zero-phonon level of the electronic state $|C\rangle$ and the phonon-continuum of state $|B\rangle$. The matrix elements turn out to be[11]

$$\langle \psi_C^0 \mid H \mid \psi_C^0 \rangle = E_C^0 \ ,$$

$$\langle \psi_C^0 \mid H \mid \psi_B^n(E) \rangle$$

$$\equiv V_n(E) = \langle \phi_C \mid H' \mid \phi_B \rangle a_{n0'} \left[\Omega = \frac{E - E_B^0}{\hbar} \right] \ , \tag{8}$$

$$\langle \psi_B^n(E_1) \mid H \mid \psi_B^m(E_2) \rangle = E_1 \delta_{mn} \delta(E_1 - E_2) \ .$$

The wave function of the interacting system has the form

$$|\psi(E)\rangle = \alpha(E) \mid \psi_C^{0'} \rangle + \sum_n \int b(E') \mid \psi_B^n(E') \rangle dE'$$

Since, according to hypothesis (5), only the $|A\rangle \rightarrow |C\rangle$ radiative transition is allowed, the intensity of the radiative transition from $|\psi_A^0\rangle$ to the state $|\psi(E)\rangle$ resulting from the diagonalization is given by

$$I(E) = \text{const} \times |\langle \phi_A \mid P \mid \phi_C \rangle|^2 \, |\alpha(E)|^2 \ , \tag{9}$$

where P is the electric or magnetic dipole operator, and $\alpha(E)$, which represents the coefficient of the discrete state $|\psi_C^{0'}\rangle$ in the perturbed state $|\psi(E)\rangle$, is given by[11]

$$|\alpha(E)|^2 = \frac{1}{2\pi} \frac{W(E)}{[E - E_C^0 - F(E)]^2 + [W(E)/2]^2} \ , \tag{10}$$

where[13]

$$W(E) = \frac{2\pi}{\hbar} \sum_n |V_n(E)|^2$$

$$= \frac{2\pi}{\hbar} |\langle \phi_B \mid H' \mid \phi_C \rangle|^2 G \left[\Omega = \frac{E - E_B^0}{\hbar} \right] \ , \tag{11}$$

and

$$F(E) = \frac{1}{2\pi} P \int dE' \frac{W(E')}{E - E'} \ , \tag{12}$$

where P means "principal part of." Equation (10) has a Lorentzian-like dependence on E, which becomes a Lorentzian when $G(\Omega) \sim$ const. In such a case, W is the width and the peak energy is shifted with respect to E_C^0 by the amount F (Lamb shift).

It may be interesting to note at this stage that the configuration-interaction approach that we have adopted deals with stationary states and as such never involves the concept of NRT. On the other hand, when $G(\Omega) \sim$ const, Eq. (11) just gives the same result as the first-order time-dependent perturbation theory, i.e., the Fermi golden rule. In this latter framework, if the system were prepared in the nonstationary state $|\psi_C^0\rangle$ at a given time, it would evolve to the continuum of vibronic states $|\psi_B^n(E)\rangle$ with a lifetime $\tau = \hbar/W$. The configuration-interaction approach, however, gives more information, i.e., the magnitude of the Lamb shift and the shape of the zero-phonon line when $G(\Omega)$ cannot be considered as constant.

For the application of Eqs. (11) and (12) to real physical systems the simple model we employed must be extended in order to take into consideration:

(1) the degeneracy of the zero-phonon discrete state $|C\rangle$, which is lifted by the spin-orbit coupling, giving rise to a quartet, and

(2) the existence of two $|B\rangle$-like states with their respective continua.

Item (1) does not cause any qualitative difference in Eqs. (11) and (12); in fact, we only have to consider the four sublevels separately as far as we may neglect second-order interaction (through the continuum) between the two discrete sublevels Γ_8 and Γ_8' which span the same irreducible representation (IR) of O_h^*; this is equivalent to neglecting quantum beats; it will be shown in the following sections that both experimental evidence and theoretical arguments justify neglecting such mixing. As for the existence of two continua, it simply requires that two different contributions to both Eqs. (11) and (12) must be summed up to obtain the actual width and shift.

III. APPLICATION OF THE SIMPLE MODEL

The low-lying electronic levels of d^3 ions in cubic symmetry are $^4A_2$ (corresponding to the ground state $|A\rangle$ of the model), ^2E and $^2T_1$ (state $|B\rangle$ of

the model), and $^4T_2$ (state $|C\rangle$ of the model). In the absorption spectrum the prominent $^4A_2 \rightarrow {}^4T_2$ transition shows a broad structured band and a zero-phonon line which, depending on the system, presents a more or less resolved spin-orbit structure (See Figs. 2 and 3 for MgO:V^{2+}). The ZPL is magnetic dipole allowed, whereas the sideband has both magnetic and electric dipole characters.[14–17] The former is known to be a spin-orbit quartet (Γ_7, Γ_8, Γ_6, and Γ_8') in $KMgF_3$:V^{2+},[18] and recent measurements on MgO:V^{2+} indicate[17,19,20] that the ZPL is the envelope of three Lorentzians whose widths and energies are reported in Table I. This deconvolution leads to the symmetry assignment reported in Fig. 3.[17]

In MgO:V^{2+} as well as in the d^3 systems that we shall consider later, the $^4T_2$ state does not emit at low temperature, indicating that fast NRT take place to $^2T_1$ and ^2E; the only observed emission is a sharp ZPL from the ^2E state, plus a negligible contribution from the relative sideband [which justifies hypothesis (4) of Sec. II]. Actually, in the cubic systems the observed sideband emission is comparable in intensity to the ZPL, but this is due to odd-vibration-induced electric dipole transitions which, for symmetry reasons, are irrelevant to our purposes.

We now compute the homogeneous broadening of the ZPL's due to interaction with the continuum of vibronic states. We will carry out the calculation for MgO:V^{2+}, where comparison with experiment is most easily feasible; the results will indicate the limits of the present model and the way to overcome them.

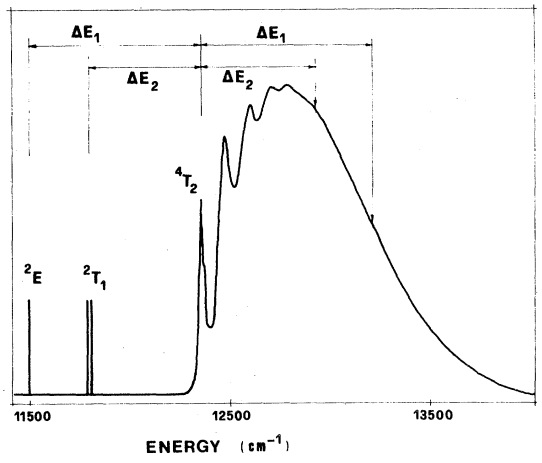

FIG. 2. Excitation spectrum of MgO:V^{2+} at $T = 8$ K. The position of the zero-phonon lines of ^2E and $^2T_1$ is reported schematically. The vertical arrows indicate the energies at which $G(\Omega)$ has to be evaluated for the calculation of the widths.

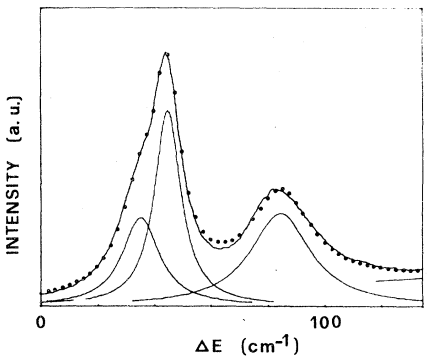

FIG. 3. $^4A_2 \rightarrow {}^4T_2$ zero-phonon line of MgO:V^{2+}. Full line, experimental excitation spectrum at $T = 8$ K (see Ref. 17); dots, fitting as sum of the three underlying Lorentzian curves.

The interaction Hamiltonian H' is the interstate spin-orbit interaction. Since H' transforms as the Γ_1^+ IR of O_h^*, it can mix only vibronic states which span the same IR. If, as in the present model, only totally symmetrical vibrations are considered, the symmetry of the vibronic states is the same as for the electronic ones. Therefore, as the IR's of $^2T_1$ are Γ_6 and Γ_8, and as the IR's of ^2E is Γ_8, it results that the Γ_7 component of $^4T_2$ is unaffected, while the Γ_8 components couple with both $^2T_1$ and ^2E continua, and Γ_6 couples only to $^2T_1$.

The matrix elements of H' are found in Griffith[21] for the cubic case as a function of the spin-orbit

TABLE I. Experimental and calculated widths (in cm^{-1}) for the $^4A_2 \rightarrow {}^4T_2$ ZPL of MgO:V^{2+}. Contributions due to the interaction between $^4T_2$ and ^2E, $^2T_1$, are reported separately. Figures in parentheses: without Jahn-Teller effect.

		Γ_7	Γ_8	Γ_6	Γ_8'
^2E		(0)	(3.0)	(0)	(27.5)
		11.3	2.2	0.02	18.2
$^2T_1$	Γ_8	(0)	(2.7)	(0)	(10.9)
		2.2	3.7	3.2	6.1
	Γ_6	(0)	(0)	(27.2)	(0)
		2×10^{-5}	4.3	14.1	0.6
Total		(0)	(5.8)	(27.2)	(38.3)
		13.5	10.2	17.3	25.0
Expt.		16	11.4	26	

constant ζ, which turns out to be 136 cm^{-1} for $MgO:V^{2+}$.[17] In order to use Eqs. (11) and (12) to compute W and F, we must know $G(\Omega)$; its calculation is the basic difficulty in calculating NRT rates, as is shown by the many attempts made in this direction.[1] However, if assumptions (3) and (4) of Sec. II are valid,[13] $G(\Omega)$ can more simply be deduced by the experimental absorption spectrum. The arrows in Fig. 2 indicate the energies at which $G(\Omega)$ must be measured for $MgO:V^{2+}$ in evaluating W. Such energies are given [see Eq. (11)] by $E_C^0 + (E_C^0 - E_B^0)$, $B = {}^2E, {}^2T_1$. Since the experimental absorption spectrum is the resultant of the magnetic dipole contribution and the vibration-allowed electric dipole one, which are shifted with respect to each other,[17] and since we must consider only the magnetic dipole band, the deconvolution procedure of Ref. 17 gives the $G(\Omega)$ we used (Pekarian, computed with $\hbar\omega = 500$ cm^{-1} and $S_0 = 1.6$). We do not expect this procedure to yield a very accurate result; however, in the spectral region indicated by the arrows, the dependence of the Pekarian curve on the relevant parameters (S_0 and $\hbar\bar{\omega}_1$) is not too strong, contrary to what would happen in the extreme tail of the spectrum. We are therefore confident that the values of $G(\Omega)$ so obtained are accurate, say, within 20%.

The results are summarized by the bracketed figures of Table I. As can be seen, the order of magnitude of the width is correctly accounted for, except for Γ_7 for which the present model gives zero width for symmetry reasons.

This indicates that non-totally-symmetrical vibrations are important in determining the width of the single components of the ZPL. In fact, the Jahn-Teller effect mixes electronic states of different symmetry, causing a redistribution of intensity[22] and width among the sublevels.

The same considerations apply to the energy shift given by Eq. (12), which is reported in Table II. In the next section we shall introduce the Jahn-Teller effect and consider the case of the other above-mentioned systems as well.

IV. ROLE OF THE JAHN-TELLER EFFECT

Let us consider now the effects which break the strict selection rules which forbid NRT among electronic states of different symmetry. Actually, such selection rules still hold for vibronic states; however, when non-totally-symmetrical vibrations are taken into account, vibronic states with the same symmetry can contain electronic states of different symmetries, which can in this way be mixed by the electronic operator H'.

More precisely, two new effects are to be expected as regards the shape of the ZPL:

(i) an internal relaxation among the spin-orbit-split components of the ZPL, and

(ii) the above-mentioned breaking of the selection rules of Sec. III.

The first effect, which concerns only the electronic state $|C\rangle$ of Fig. 1, corresponds to a thermalization among the different spin-orbit components. In the configuration-interaction picture this process is due to resonance among the higher-energy components of the ZPL and the sidebands relative to the lower-energy ones; the magnitude of the effect depends on the spin-orbit splittings and on the density of vibrational states of the right symmetry at the energies of interest. In cases where the spin-orbit splitting is of the same order of magnitude as the Debye frequency of the crystal, the effect could be very pronounced and the high-energy components of the ZPL could be as broad as to be uneasily detected. This could be the case of the ${}^4T_2$ state of $Cs_2SiF_6:Mn^{4+}$,[23] and of ${}^5T_2$ of $MgO:Fe^{2+}$,[24] where the high-energy components of the ZPL are not observed. On the other hand, where the overall splitting is of the order of 50 cm^{-1} or less, (or when, like in V^{2+} the spin-orbit constant is not very high), only low-energy acoustic phonons can produce

TABLE II. Experimental and calculated splittings for the ${}^4A_2 \rightarrow {}^4T_2$ ZPL of $MgO:V^{2+}$. All data in cm^{-1}.

IR	Expt	Splittings Calc [a]	Calc [b]	Lamb shift
Γ_7	0	0	0	8.2
Γ_8	10	14.4	18.6	4.0
Γ_6	50	42.8	45.0	6.0
Γ_8'		56.0	43.8	20.4

[a]With Lamb shift.

[b]Without Lamb shift (see Ref. 17).

broadening. The effects to be expected are not very clear, but some information can be obtained from the absorption spectrum of $KMgF_3:V^{2+}$, where this is the only homogeneous broadening mechanism of the ${}^4A_2 \rightarrow {}^4T_2$ ZPL, ${}^4T_2$, being the first excited state. As can be seen from Sturge's data[18] the ZPL's are not very broad: ~ 2 cm^{-1} for the lowest-energy one and ~ 5 cm^{-1} for the highest-energy one; the width increase is in qualitative agreement with the previous discussion. Also, the width (~ 5 cm^{-1}) of the highest-energy component gives an upper limit to the combined effects of mechanism (i), plus inhomogeneous broadening.

Since the observed widths in $MgO:V^{2+}$, $MgO:Cr^{3+}$, and $Al_2O_3:Cr^{3+}$ are larger by about 1 order of magnitude, we feel confident in neglecting mechanism (i), even though in principle one would have to be sure that the density of vibrational states does not change much in the range of interest.

The preponderance of mechanism (ii) over mechanism (i) means that NRT from ${}^4T_2$ to ${}^2T_1$ and ${}^2E$ are fast enough not to allow the system to thermalize within ${}^4T_2$. It should also be noted that the pseudo-Jahn-Teller effect between states $|B\rangle$ and $|C\rangle$ cannot induce NRT by itself because of the different spin multiplicities of these states.

In the present case, the Hamiltonian is given by

$$H = H_0 + H_{JT} + H' \ , \tag{13}$$

where H_0 contains all of the adiabatic terms including the first-order spin-orbit interaction within $|C\rangle$, H' is the interlevel spin-orbit interaction, and H_{JT} is the Jahn-Teller Hamiltonian relative to ϵ_g modes, which have prominent coupling[14,17] in the system we are considering. We still use hypothesis (4) of Sec. II, so that H_{JT} operates only on state $|C\rangle$, in agreement with experimental evidence.[14,25]

We now carry out the same calculation as in Sec. II, taking for zero-order wave functions the eigenfunctions of $H_0 + H_{JT}$. The vibronic eigenfunctions and eigenvalues of H_0 are

$$|\psi_{\Gamma\gamma}\rangle = |[\phi_R \otimes n_\epsilon(\Omega_\epsilon)]_{\Gamma\gamma}\rangle\, |n_1(\Omega_1)\rangle \ , \tag{14}$$

$$E_{\Gamma\gamma} = E_R + \hbar\Omega_\epsilon + \hbar\Omega_1 \ , \tag{15}$$

where Γ and γ are, respectively, the IR of the double group and its component, spanned by the vibronic state, R is the IR of the electronic state, $|n_\epsilon(\Omega_\epsilon)\rangle$ is the symmetrized vibrational wave function relative to the Jahn-Teller-active modes which span the ϵ irreducible representation, $|n_1\rangle$ is the vibrational wave function relative to the totally symmetrical mode, and the symbol $\otimes$ indicates symmetrized product. The wave functions of Eq. (14) represent, on the one hand, the continuum states relative to $|B\rangle$; on the other hand, they represent the starting wave functions relative to $|C\rangle$ before H_{JT} is applied. The $H_0 + H_{JT}$ wave functions of the ZPL of $|C\rangle$ are

$$|\psi^C_{\Gamma\gamma}\rangle = \left[\sum_{R=\Gamma} b_{00'}^{\Gamma R}\, |\phi^C_{R\gamma}\rangle\, |0_\epsilon\rangle + \sum_{Rn_\epsilon} \int d\Omega_\epsilon b_{0n'}^{\Gamma R\epsilon}(\Omega_\epsilon)[\,|\phi^C_R\rangle \otimes |n_\epsilon(\Omega_\epsilon)\rangle]_{\Gamma\gamma}\right] \times \left[a_{00'}\,|0_1\rangle + \sum_{n_1} \int d\Omega_1 a_{0n'}(\Omega_1)\,|n_1(\Omega_1)\rangle\right] \ , \tag{16}$$

where the first sum over R is extended to the electronic states such that $R = \Gamma$ (in the case of ${}^4T_2$, $R = \Gamma_8, \Gamma'_8$, if $\Gamma = \Gamma_8$; in the case of Γ_6 and Γ_7 the sum reduces to only one term), $b_{00'}^{\Gamma R}$ and $b_{0n'}^{\Gamma R\epsilon}$ have the same meaning, for Jahn-Teller-active modes, as have a_{00} and a_{0n} in Sec. II.

The matrix elements of H' analogous to those of Sec. II [Eq. (8)] between $|\psi^C_{\Gamma\gamma}\rangle$ and the states $|\psi^B_{\Gamma\gamma}(n_\epsilon n_1)\rangle$ of Eq. (14) are given by

$$\langle\psi^B_{\Gamma\gamma}(n_\epsilon n_1)\,|H'|\,\psi^C_{\Gamma\gamma}\rangle = \sum_R b_{0n'}^{\Gamma R\epsilon}(\Omega_\epsilon) a_{0n'}(\Omega_1)\langle\phi^B|H'|\phi^C_R\rangle \ . \tag{17}$$

Since both H_{JT} and H' are independent on γ, Eq. (17) is appropriate for every γ. In the case $n_\epsilon = 0$, Eq. (17) becomes

$$\langle\psi^B_{\Gamma\gamma}(0n_1)\,|H'|\,\psi^C_{\Gamma\gamma}\rangle = \sum_{R=B} b_{00'}^{\Gamma R} a_{0n'}(\Omega_1)\langle\phi^B|H'|\phi^C_R\rangle \ . \tag{18}$$

The contributions from different continua to the line shape of Eq. (10) are additive, such that Eq. (10) still holds with $W(E) = W_1(E) + W_\epsilon(E)$, where

$$W_1(E) = \frac{2\pi}{\hbar} \left| \sum_R b_{00'}^{\Gamma R} \langle \phi^B | H' | \phi_R^C \rangle \right|^2 \times G_1 \left[\Omega_1 = \frac{E - E_B^0}{\hbar} \right] , \tag{19}$$

and

$$W_\epsilon(E) = \frac{2\pi}{\hbar} \sum_{n_\epsilon} \int d\Omega_\epsilon G_1 \left[\Omega_1 = \frac{E - E_B^0}{\hbar} - \Omega_\epsilon \right] \times \left| \sum_R b_{0n'}^{\Gamma R \epsilon}(\Omega_\epsilon) \langle \phi^B | H' | \phi_R^C \rangle \right|^2 . \tag{20}$$

Equation (19) represents the contribution by totally symmetrical vibrations alone and resembles the result obtained in in Sec. II. Equation (20) is the main new contribution of the Jahn-Teller effect, mechanism (ii). As regards the energy shift, Eq. (12) is still valid if the substitution $W(E) = W_1(E) + W_\epsilon(E)$ is made.

Let us now test the theory we have developed [Eqs. (12), (19), and (20)] on physical systems. We shall start with $Al_2O_3:Cr^{3+}$; in this system the Jahn-Teller effect is rather strong, such that no spin-orbit structure is observed in the ZPL of the $^4A_2 \rightarrow {}^4E$ ($^4T_2$) transition, which should in principle be a quartet.[25] This implies that the electronic states are strongly (and roughly equally) mixed in each of the four zero-phonon vibronic states. In such a situation, the four ZPL's are expected to be more or less equally broadened and the width can be computed as in Sec. II, provided the squared matrix element of the interaction Hamiltonian H' is averaged over the spin-orbit substates of $|C\rangle$. For the calculation, the value $\zeta = 170$ cm^{-1} has been used[25]; as regards $G(\Omega)$, the values of the energy levels are well known and $G(\Omega)$ has been evaluated from the $^4A_2 \rightarrow {}^4T_2$ absorption spectrum of Ref. 26. $G(\Omega)$ can also be evaluated by assuming a Pekarian shape and using the parameter values of Ref. 9; the value one obtains in this way agrees within 10% with the experimental one.

The overall width we obtain is 31.6 cm^{-1}, of which 19.8 cm^{-1} is due to interaction with ^2E and 11.8 cm^{-1} to interaction with $^2T_1$. The corresponding transition rates are 3.7×10^{12} and 2.2×10^{12} sec^{-1}, respectively. The width of 31.6 cm^{-1} that we find compares very well with the low-temperature experimental value[26] of ~ 45 cm^{-1}, also in view of the fact that the computed value is actually the average width of one component and no account has been taken of possible spin-orbit splitting of the components; this latter effect makes the experimental ZPL look broader. Therefore, our results are in agreement with those of Ref. 6, which show that the ZPL is predominantly homogeneously broadened.

The present results should be compared with previous calculations carried out within different frameworks.[9,27] The calculations of Ref. 27, made under the assumption that the $^4T_2 \rightarrow {}^2E$ NRT proceed via the intermediate $^2T_1$ level, neglecting the direct $^4T_2 \rightarrow {}^2E$ process, give a transition rate of $\sim 10^{10}$ sec^{-1}, which is too small by more than 2 orders of magnitude. As regards the comparison with the results of the simple model of Ref. 9, the main difference is that those authors find the $^4T_2 \rightarrow {}^2T_1$ rate to be larger than $^4T_2 \rightarrow {}^2E$. This is due to their assumption that the matrix element of H' is the same for all states and that it can be handled as a fitting parameter. In this way all of the NRT rates are proportional to the vibrational overlap integrals. Actually the strength of the spin-orbit interaction (average squared matrix element) with ^2E is more than twice as much as with $^2T_1$. Also, the total NRT rate from $^4T_2$ of Ref. 9 is larger by 1 order of magnitude than the experimentally deduced one.

Let us now turn to systems on which the theory of the present section, including the Jahn-Teller effect, can be tested more directly. Among these, $MgO:V^{2+}$ is particularly well suited because the Jahn-Teller effect is active in the $^4T_2$ excited state but the quenching it operates on the spin-orbit interaction[28] is rather weak and the spin-orbit structure can be observed (Fig. 3). The Jahn-Teller effect in this system has been studied by taking into account ϵ modes in Ref. 17, within the single-mode picture. In order to fit the splittings and the relative intensities of the components of the ZPL the following parameter values were used: $E_{JT} = 100$ cm^{-1}, $\hbar\omega_\epsilon = 200$ cm^{-1}, $\zeta = 136$ cm^{-1}, where ω_ϵ has the meaning of an effective frequency. Second-order spin-orbit effects, mainly due to interaction with ^2E and $^2T_1$, were taken into account by an effective Hamiltonian. What emerges is that the totally symmetrical modes have the prominent coupling. This suggests a way of simplifying Eq. (20) through a simplification of the wave function of Eq. (16), which consists of building up $|\psi_{\Gamma\gamma}^C\rangle$ with ϵ_g phonons having all the same frequency, instead of a continuum distribution which would make the Jahn-Teller problem almost untractable. This can be justified by considering that the coupling to Γ_1^+ modes is ~ 10 times stronger than to ϵ_g modes,

such that Eq. (16) will contain essentially, say, $|0_\epsilon\rangle$ and $|1_\epsilon\rangle$ vibrational functions and many-phonon Γ_1^+ vibrational functions. Since the energy gaps $^4T_2-{}^2T_1$ and $^4T_2-{}^2E$ are of the order of $1000-2000$ cm^{-1}, the NRT involve several Γ_1^+ phonons, which have a continuum of frequencies and are sufficient to ensure resonance. The effect of ϵ_g modes is just to couple different spin-orbit substates of $^4T_2$, and substitution of the continuum distribution by a single frequency is not expected to cause strong differences. This assumption has been checked by repeating the calculation with two different ϵ_g frequencies (200 and 300 cm^{-1}); the results were reproducible within 10%.

The assumption of a single Jahn-Teller-active mode of frequency corresponds to taking

$$b_{0n'}^{\Gamma R\epsilon}(\Omega_\epsilon) = b_{0n'}^{\Gamma R\epsilon}\delta(\Omega_\epsilon - \omega_\epsilon) \tag{21}$$

in Eq. (20), which becomes

$$W_\epsilon(E) = \frac{2\pi}{\hbar}\sum_{n_\epsilon}\left|\sum_R b_{0n'}^{\Gamma R\epsilon}\langle\phi^B|H'|\phi_R^C\rangle\right|^2 \times G_1\left[\Omega_1 = \frac{E-E_B^0}{\hbar} - n_\epsilon\omega_\epsilon\right] . \tag{22}$$

The coefficients $b_{00'}$ of Eq. (19) and $b_{on'}$ of Eq. (22) are obtained by diagonalizing numerically the Hamiltonian $H_0 + H_{JT}$. In order to evaluate G_1, we have assumed a continuous Pekarian shape. The value of S_0 is now reduced with respect to the calculation of Sec. II ($S_0 = 1.6$) to take into account that now part of the energy lowering of the $^4T_2$ zero-phonon state is due to ϵ_g modes

$$S_0\hbar\bar{\omega}_1 + E_{JT} = 800 \text{ cm}^{-1} . \tag{23}$$

Taking $\hbar\bar{\omega}_1 = 500$ cm^{-1} (see Sec. III), Eq. (23) gives $S_0 = 1.3$ for $E_{JT} = 150$ cm^{-1} ($\hbar\omega_\epsilon = 300$ cm^{-1}) and $S_0 = 1.4$ for $E_{JT} = 100$ cm^{-1} ($\hbar\omega_\epsilon = 200$ cm^{-1}).[17]

The results for the various widths and shifts, relative to the first choice of the parameters, are given in Tables I and II. As expected, the sum of the widths (taking into account degeneracy) is not changed by the Jahn-Teller effect, but this latter causes a redistribution of the width among the various levels, bringing the calculated widths into very good agreement with experiment. It might be surprising that Γ_7, which is not broadened without the Jahn-Teller effect, becomes broader than Γ_8; this is due to interference in Eq. (22) among spin-orbit and Jahn-Teller contributions; such interference is constructive for Γ_7 and destructive for Γ_8. A similar kind of destructive interference makes the Γ_8-Γ'_8 mixing very small, as evidenced by magnetic circular dichroism (MCD) measurements,[19,20] and as it results from the calculations of Ref. 17.

The shifts and the final energies of the levels (including spin-orbit splitting) are reported in Table II. It should be noted that all levels are shifted towards high energy, but Γ_6 and Γ'_8 more so than Γ_7 and Γ_8. For comparison the results of Ref. 17 [calculation (b)], where $H_{JT} + H_{SO} + H_{SO}^{(2)}$ were diagonalized together but with no account of Fano resonances, are reported. The present results are in better agreement with experiment, especially as regards the unexpected coincidence of Γ_7 with Γ_8. In fact, on the basis of Ham's theory the ratio $[E(8') - E(8)]/[E(8) - E(7)]$ should be ~ 1.67, whereas the experimental value is 4. The interaction with the continuum of states accounts for such a strong second-order spin-orbit effect. In this way the origin of the anomalies of MgO:V^{2+} with respect to $KMgF_3$:V^{2+}, where Ham's theory[29] is able to correctly explain the observed splittings, becomes clear. In fact, it appears that when there is interaction between the discrete and continuum states the second-order spin-orbit interaction, which causes the Lamb shift, must be properly taken into account. In $KMgF_3$:V^{2+} no such problem arises because $^4T_2$ is the lowest excited state and there are no NRT, the lines are much sharper, and Ham's theory works well.

Let us now consider other systems (Cs_2SiF_6:Mn^{4+} and MgO:Cr^{3+}) whose spectra are even more anomalous than those of MgO:V^{2+}. As regards Mn^{4+}, the experimental spectrum for $^4A_2 \rightarrow {}^4T_2$ ZPL shows only two components whose widths are 5 cm^{-1} (Γ_7) and 8 cm^{-1} (Γ_8).[23] The Γ_6 and Γ'_8 components are only observed as weak peaks in MCD.[23] In order to compute the widths we have used the following parameter values: $\hbar\omega_1 = 600$ cm^{-1}, $\hbar\omega_\epsilon = 512$ cm^{-1}, $E_{JT} = 546$ cm^{-1}, $\zeta = 380$ cm^{-1}, and $G(\Omega)$ has been deduced from the spectrum of Ref. 23. The calculated widths are, in cm^{-1},0 (Γ_7), 2.3 (Γ_8), 13 (Γ_6), and 15 (Γ'_8) without the Jahn-Teller effect, 5 (Γ_7), 7 (Γ_8), 9 (Γ_6), and 10 (Γ'_8) with the Jahn-Teller effect. In this system the Jahn-Teller effect is quite strong and its result is to redistribute the widths more or less uniformly among the various Γ's (similar to Al_2O_3:Cr^{3+}). On the other hand, the computed values with the JTE can only give the correct

order of magnitude, because in this case Eq. (21) is not a good approximation, since due to the strong JTE, many ϵ_g phonons are involved in the nonradiative transition and it is not correct to neglect their frequency dispersion. Moreover, $G(\Omega)$ is not a smooth function in the frequency range of interest. It is important, however, that the computed widths of Γ_7 and Γ_8 are in agreement with the experimental ones, especially in view of the remarkable differences between these parameters and those of $MgO:V^{2+}$. In fact $\zeta(Mn^{4+}) \sim 3\zeta(V^{2+})$, while the values of $G(\Omega)$ are in the present case smaller by 1 order of magnitude because here $6-8$ phonons are involved, contrary to $MgO:V^{2+}$ where only $2-3$ are involved. As regards Γ_6 and Γ'_8, the fact that these states are not observed in the spectrum is still an open problem; one of the reasons may be a further broadening due to processes not considered here such as internal relaxation among the spin-orbit-split components.

The same kind of calculation has been carried out for $MgO:Cr^{3+}$. In this case, also, the simplifying assumptions of Eqs. (21) and (22) are less valid, because the energy gap $^4T_2-{}^2T_1$ is only $\sim 500\ cm^{-1}$, such that one-phonon processes are favored and the results are strongly dependent on the shape of the one-phonon densities of states of different symmetries. In this case the calculation including the JTE could not be carried out because E_{JT} is not deducible from the ZPL, whose structure has not yet been well unraveled.[16] The results for the computed widths without JTE, in cm^{-1}, are 0 (Γ_7), 30 (Γ_8), 80 (Γ_6), 230 (Γ'_8).

Even though the JTE would redistribute the widths among the various levels, such widths are unexpectedly large if the structure of the ZPL of $MgO:CR^{3+}$ had the same origin as in $MgO:V^{2+}$, as hypothesized in Ref. 16. More accurate experimental investigation is required. On the other hand, such large widths as $230\ cm^{-1}$, which are comparable with the phonon energies, cast doubts on the applicability of Fano's theory, which is a perturbative one.

V. CONCLUSIONS

In general, the theoretical treatment of NRT in solid-state impurities is a complicated matter, such that even the correct order of magnitude is difficult to obtain. In contrast, in the systems we have considered, the situation is more favorable both experimentally and theoretically; in fact, quite strong spin-orbit coupling causes the ZPL to be rather broad and a direct experimental observation of the nonradiative transition rates is possible, if one is able to distinguish between homogeneous and strain-induced inhomogeneous broadening. On the other hand, the spin-orbit operator, whose effect is more important than other nonadiabatic effects, can be quite easily handled. Moreover, large vibrational overlaps, due to the smallness of the electronic energy gaps, make anharmonic effects less important than in other systems.[10] Such overlaps can either be deduced directly from the optical spectra or be calculated by simple models.

This situation allows the Jahn-Teller effect to be taken into account in a simplified way. This is an important point because the symmetry breaking introduced by the JTE is necessary to explain in detail the width and shift of the various components of the ZPL.

It should be noted that in our calculations we made use of no independent fitting parameter; nevertheless, the agreement we obtain for $MgO:V^{2+}$ and $Al_2O_3:Cr^{3+}$ is excellent and the differences between observed and calculated values are largely accounted for by the uncertainty of parameter values. Previous calculations[9,27] could not give the correct order of magnitude.

The present model, together with the intensity-quenching effect,[17,22] satisfactorily explains the long-questioned[14,17,19,29,30] structure of $MgO:V^{2+}$ zero-phonon line. As regards $Cs_2SiF_6:Mn^{4+}$ our model reproduces correctly the widths of the two observed lines, but it is clearly inadequate to explain the disappearance of the other two; this effect must be caused by some different mechanism. In the case of $MgO:Cr^{3+}$, the present model predicts very large widths for Γ_6 and Γ'_8. At the present time such prediction is neither confirmed nor refuted by experiment.

The main limits of the present treatment are the same as those of the theory of the JTE, i.e., the problem becomes intractable if one wishes to consider a continuum of Jahn-Teller-active modes. Furthermore, our assumption of no Γ_8-Γ'_8 interaction is no longer valid when these peaks are superimposed or nearly so.

ACKNOWLEDGMENTS

This work was supported in part by the Consiglio Nazionale delle Ricerche, Contratto No. 80.02409.02. The authors wish to thank Dr. E. Sigmund and Professor M. Wagner for helpful discussions.

[1]R. Englman, *Nonradiative Decay of Ions and Molecules in Solids* (North-Holland, Amsterdam, 1979), and references therein.
[2]F. K. Fong, *Theory of Molecular Relaxation* (Wiley, New York, 1975).
[3]A. M. Stoneham, *Theory of Defects in Solids* (Clarendon, Oxford, 1975).
[4]See, for instance, *Radiationless Processes*, edited by B. DiBartolo (Plenum, New York, 1980).
[5]M. Montagna, O. Pilla, and G. Viliani, Phys. Rev. Lett. 45, 1008 (1980).
[6]A. Monteil and E. Duval, J. Lumin. 18-19, 793 (1979).
[7]R. Englman and R. Barnett, J. Lumin. 3, 37 (1970).
[8]R. Barnett and R. Englman, J. Lumin. 3, 55 (1970).
[9]W. H. Fonger and C. W. Struck, Phys. Rev. B 11, 3251 (1975).
[10]M. D. Sturge, Phys. Rev. B 8, 6 (1973).
[11]U. Fano, Phys. Rev. 124, 1866 (1961).
[12]U. Fano and J. W. Cooper, Rev. Mod. Phys. 40, 441 (1968).
[13]Strictly speaking, $G(\Omega)$ as it appears in Eq. (11) is not exactly the same as defined in Eq. (6). This can be seen from Eq. (8), where $a_{n0'}$ appears instead of $a_{0n'}$ as in Eq. (6). However, within the linear coupling approximation these two quantities are equal and Eq. (11) introduces no ambiguity. If the linear coupling approximation were released, six different G's should be introduced, one for each possible absorption and emission transition among the electronic states. The one to be inserted in Eq. (11) would be $G_{C\text{-}B}$. In the systems we shall be concerned with, the only experimentally observable G's at low temperature are $G_{A\text{-}C}$, $G_{A\text{-}B}$, and $G_{B\text{-}A}$.
[14]M. D. Sturge, Phys. Rev. 140, A880 (1965).
[15]B. DiBartolo and R. Peccei, Phys. Rev. 137, A1770 (1965).
[16]A. Boyrivent, E. Duval, M. Montagna, G. Viliani, and O. Pilla, J. Phys. C 12, L803 (1979).
[17]G. Viliani, O. Pilla, and M. Montagna, Phys. Rev. B 23, 18 (1981).
[18]M. D. Sturge, Phys. Rev. B 1, 1005 (1970).
[19]G. Viliani, M. Montagna, O. Pilla, A. Fontana, M. Bacci, and A. Ranfagni, J. Phys. C 11, L439 (1978).
[20]N. B. Manson and M. D. Sturge, Phys. Rev. B 22, 2861 (1980).
[21]J. S. Griffith, *The Theory of Transition-Metal Ions* (Cambridge University, New York, 1961).
[22]M. Montagna, O. Pilla, and G. Viliani, J. Phys. C 12, L699 (1979).
[23]N. B. Manson, Z. Hasan, and C. D. Flint, J. Phys. C 12, 5483 (1979).
[24]F. S. Ham, W.M. Schwarz, and M. C. M. O'Brien, Phys. Rev. 185, 548 (1969).
[25]W. M. Fairbank and G. K. Klauminzer, Phys. Rev. B 7, 500 (1973).
[26]J. Margerie, C. R. Acad. Sci. 257, 2634 (1962); thesis, Université de Paris, 1965 (unpublished).
[27]Yu. E. Perlin, B. S. Tsukerblat, and E. I. Perepelitsa, Zh. Eksp. Teor. Fiz. 62, 2265 (1972) [Sov. Phys.—JETP 35, 1185 (1973)].
[28]F. S. Ham, Phys. Rev. 138, A1727 (1965).
[29]F. S. Ham, in *Optical Properties of Ions in Solids,* edited by H. M. Crosswhite and H. W. Moss (Wiley, New York, 1967), p. 357.
[30]A. Ranfagni and G. Viliani, Phys. Status Solidi B 84, 393 (1977).